



# Computational Analysis of Pressure Distribution of Traditional Aceh Boat Hull Attributed to Speed Variations

Y. Muchlis<sup>1,2</sup>, Husaini<sup>1,3</sup>, N. Ali<sup>1,3</sup>, Akhyar<sup>1,3,\*</sup>, A. Tamlicha<sup>3</sup>

## ARTICLE INFO

### Article history:

Received 29 Jul 2024;  
in revised from 31 Jul 2024;  
accepted 15 Aug 2024.

### Keywords:

Computational Analysis, Traditional Aceh Boat, Hull, Hydrodynamic Performance, Speed Variations.

## ABSTRACT

Computational fluid dynamics (CFD) is widely applied in the shipping industry to analyze fluid flow in predicting hull pressure due to water. This analysis facilitates a comprehensive understanding of pressure distribution along the hull when design changes are implemented to withstand hydrodynamic pressure during operation. In recent years, applications for composite hull materials have gained significant attention for investigation. For a wide range of applications, both civil and military, precise information regarding the loading force acting on the hull surface and the shape of the wet area is required. Therefore, this research aimed to assess the pressure distribution occurring in the hull and keel of the boat starting from the bow of the sharp area to the stern, assuming speed variations at 5.83, 11.66, 17.50, 23.33, 29.16, 34.99, 40.82, and 46.65 knots. For analysis, a traditional fishing boat shape from Aceh, Indonesia was selected. The results showed that the highest pressure occurred at the bow sharp end of the boat, reaching 259 kPa at a speed of 46.65 knots. Generally, the tendency of pressure distribution commenced at the bow of the sharp tip towards the stern due to changes in the given speed variation.

© SEECMAR | All rights reserved

## 1. Introduction.

Fishing boat is the main means for fishermen, playing an essential role in daily activities for meeting fishing needs. In the fishing boat industry, current technological developments are crucial to improve operational efficiency and safety. A crucial focus of technology in this industry is directed toward analyzing the distribution of water pressure on the hull of the boat, which significantly impacts hydrodynamic resistance and fuel consumption. The pressure of the hull is affected by the interaction between the water and the surface of the hull, which is included in the category of complicated when solved by conventional methods.

Numerical analysis for various complex conditions in several engineering applications has been successfully predicted and completed through the application of finite element methods and CFD analysis (Hasanuddin et al., 2017; Harun et al., 2021; Iqbal et al., 2021; Husaini et al., 2023).

The CFD method has become an essential tool for understanding and optimizing the distribution of pressure on the hull. Furthermore, the CFD numerical simulations offer designers a streamlined method to analyze the fluid behavior around the boat, pressure distribution, hydrodynamic forces, and the performance of the proposed boat design. Previous research has shown the effects of the hull geometry, speed, and operational conditions on the hydrodynamic pressure of a vessel's performance. The hydrodynamic characteristics of prismatic and flat plane surfaces, including lift, drag, wet area, pressure center, and plane surface stability limits, have been extensively explored regarding speed, balance angle, dead angle, dead angle, and loading (Savitsky, 1964). Calculating aerodynamic drag over the cross-sectional area of the prismatic hull above the water surface, location, size, and geometry of spray strips, buttock

<sup>1</sup>Doctoral Program, School of Engineering, Universitas Syiah Kuala, Jl. Syech Abdurrauf No. 7, Darussalam, Banda Aceh, 23111, Indonesia.

<sup>2</sup>Department of Mechanical Engineering, Universitas Abulyatama, Banda Aceh, Indonesia.

<sup>3</sup>Department of Mechanical Engineering, Universitas Syiah Kuala, Jl. Syech Abdurrauf no.7 Darussalam, Banda Aceh 23111, Indonesia.

\*Corresponding author: Akhyar. E-mail Address: akhyar@usk.ac.id.

line equilibrium angle, and average wet length have predicted three separate towing tank facilities. Aerodynamic drag, the cross-sectional area of the hull above the water level, is also calculated and included in the final performance prediction method (Savitsky et al., 2007).

Numerical simulation of free surface flow with the RANSE Volume of Fluid (VOF) solver has been used in composite hull to evaluate complex flows. Moreover, physical phenomena such as spray strips, breakwaters, trapped air, and turbulent boundary layers have been compared to Savitsky's semi-empirical methods (Caramatescu et al., 2016).

Solving the numerical flow around a planing hull based on the theory of potential flow has been addressed in several investigations (Wackers et al., 2009; Ghassemi et al., 2008). However, these methods are limited to high-velocity simulations and cannot accurately capture wave and spray curtain formation. The ensuing solutions were developed based on fresh methods for dealing with big, multi-phase Froude numbers. According to Battistin et al. (2003) and Yumin et al. (2012), the components of viscous and pressure resistance in these circumstances are nonlinearly associated with hydrodynamic lifting forces and trim angle (Azcueta, 2003).

The Reynolds-Averaged Navier Stokes equations (RANS) are used for estimating the hydrodynamic performance, the VOF method is used for estimating the free surface of an incompressible and non-miscible liquid with the second fluid (Caponetto, 2001), (Queutey et al., 2007), and the k-omega turbulence model are the foundation of the calculation model used by simulation (Kornev and Abbas, 2018).

Complex problems affected by various phases cannot be solved by analytical methods, such as dynamic pressure estimation, maps of distribution on wet surfaces, and the position of free surfaces. Typically, pressure distribution on the hull is usually estimated following registration regulations or the ISO standard (ISO 12215-5 for small boat structures), as reported by Soupez (2019). Previous research has extensively covered simulations of pressure distribution on the hull and boat considering several factors such as speed, cargo, and passengers. Despite the information available, the unique shape and design of a traditional Aceh boat have not been thoroughly evaluated, particularly to observe the amount of pressure distribution on the hull. Therefore, this research aimed to investigate the use of computational CFD in modeling pressure distribution on the hull due to speed variations to improve the efficiency and performance of the traditional Aceh boat. The novelty is that there has been no previous CFD simulation to analyze the pressure distribution on the traditional Aceh boat due to speed variations, specifically 5.83, 11.66, 17.50, 23.33, 29.16, 34.99, 40.82, and 46.65 knots.

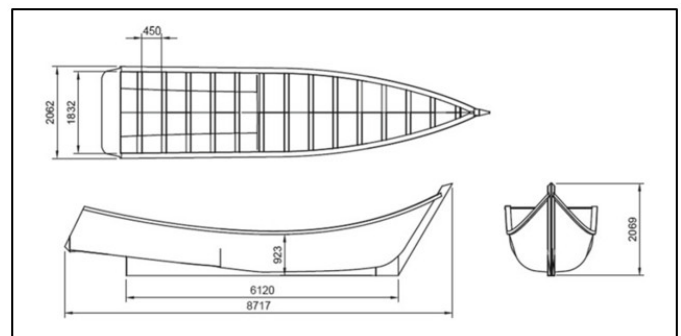
Results are expected to provide insight into vessel design strategies suitable for optimizing pressure distribution, reducing hydrodynamic resistance, and improving the performance of the Aceh boat. This analysis will make a positive contribution to the development of more efficient and environmentally friendly boat designs. Moreover, free surface flow around the boat is applied using the Volume of Fluid (VOF) approach.

## 2. Procedures.

The simulation focused on a traditional fishing boat with the hull made of fiber composite (fiberglass), characterized by a keel beam starting from the bottom back and continuous forward and curved upwards, with a width of 2,062 m and a total length of 8,717 m. A hereditary design from ancestors with wood materials was used to stabilize small boat when hitting large waves in the Indian Ocean.

Several speed variations of the fishing boat were used, ranging from 5.83 knots to the maximum of 46.65 knots, with an additional stationary condition at 0 knots, serving as a benchmark for comparison. The specific speed variations in the speed of the traditional Aceh boat given in this CFD simulation modeling are 5.83, 11.66, 17.50, 23.33, 29.16, 34.99, 40.82, and 46.65 knots. The selection of boat speed represents the operational condition, starting with 0 knots, showing a stationary condition. Subsequently, the boat began to move and the pressure on the hull was analyzed with speed intervals every 5.83 knots up to a maximum of 46.65 knots. These eight-speed intervals were selected and expected to represent the actual conditions. When the intervals were excessively narrow, the speed did not capture pressure change in the hull. However, at a wider interval, an increase in the gap of water pressure information on the hull was observed due to the effect of speed variations. The body plan of the traditional Aceh boat with a general hull size is shown in Table 1. The detailed size and shape of the main characteristics of this traditional fishing boat and the water line on the hull are shown in Figure 1.

Figure 1: Traditional Aceh fishing boat: upper, front, and side perspectives in schematic form in mm.

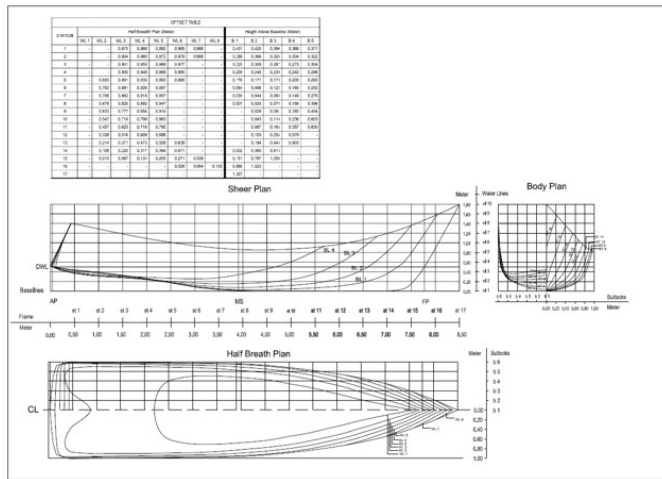


Source: Akhyar et al., 2021.

Previous simulation has carried out finite element analysis to predict stress, strain, and displacement on the traditional Aceh boat with three load variations. In addition to varying the load, it also varies four different boat wall thicknesses to predict stress, strain, and displacement (Akhyar et al., 2021). In this advanced simulation, mapping the distribution of pressure on the hull of the Aceh boat with fiberglass material was carried out at the Computational Mechanics Laboratory of the Department of Mechanical Engineering, Syiah Kuala University. Currently, the hull material of this traditional Aceh boat is usually made of wood and fiberglass and is widely used in Aceh Province,

specifically for small-sized fishing vessels, with a gross tonnage of around three GT.

Figure 2: Body plan of a Traditional Aceh fishing boat showing the hull form.



Source: Authors.

Table 1: The boat’s primary characteristics as used in the CFD simulation.

	Value
Length overall	8.717 m
Maximum beam (breadth)	2.062 m
Keel	6.120 m
Depth	2.069 m
Empty draft	0.27 m
Hull weight	220 kg
Max displacement	600 kg
Power	29.83 kW

Source: Authors.

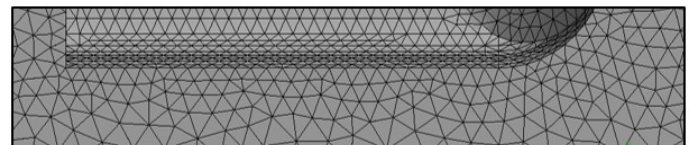
Simulation planning was carried out using NUMECA FineMarine (Caramatescu and Mocanu, 2019). The CFD simulation for Aceh fishing boat hull using the NUMECA FineMarine application included several steps such as vessel geometry modeling, mesh manufacturing, determination of boundary conditions, and completion of numerical fluid equations. Furthermore, the computational method RANS (Reynolds-Averaged Navier-Stokes) was used to analyze the distribution of pressure on the hull of ships. The geometric model of the hull of a traditional Aceh fishing boat was modeled with a Computer-Aided Design (CAD) application. Dynamic conditions such as trim and heave were left free, while the other motions were fixed based on solver specification. Subsequently, the  $k-\epsilon$  turbulence model was used to simulate the effects of turbulence around the hull of the boat. Mesh generation included structural and volume meshes for vessel walls and fluids, respectively. To discretize the hull surface, an unstructured monobloc Cartesian network was carried out. The grid has an H-H type struc-

ture consisting of adjacent tetrahedral units, averaging 2.5 million cells for the hull surface with variations in velocity values and the computational field. The selection of an unstructured monobloc Cartesian grid with an HH-type structure for simulating the traditional Aceh boat hull was driven by the need for adaptability to complex geometries, efficient mesh generation, and the ability to centralize resolution in critical areas. These features contributed to the accuracy and efficiency of simulations, particularly in capturing intricate fluid flows around the hull. Considering the primary, intermediate, and finish layers, including base material as a single-layer (un-layered), limit conditions were established on the hull surface. These included speed limit conditions, pressure, viscosity, inlet, outlet, and all other relevant limits. Finally, pressure distribution was visualized in the form of pressure contours along the surface line of the hull.

Refinement grids are used to increase cell density in specific areas of interest by dividing cells, such as free surfaces in the area of water contact with the hull of a vessel (Battistin et al., 2003). The bow and stern areas are smoothed, as shown in Figure 3. The coefficient of the non-dimensional wall function is set to  $y^+=5$  for an accurate description of the turbulent layer, considering the grid capacity available for the simulation process.

For each boat speed, a hexahedral mesh with an average size of 2.5 million cells has been constructed, as shown in Figure 3. The applied limit conditions include a constant speed equal to the ship when entering the computing plane (upstream). Shear conditions are used when the fluid exits the computational plane (downstream) and at the outer boundary of the domain. Additionally, this condition is applied to free surfaces and symmetrical planes, requiring adhesion of the fluid to the surface walls of the hull (non-slippery). By dividing cells, grid refinement creates regions of interest with higher cell densities, such as free surfaces in the area of contact with the hull (Battistin et al., 2003).

Figure 3: Mesh division to further refine regions of interest for turbulent flow phenomena.



Source: Authors.

Both the continuity equation and the Navier-Stokes equations describe fluid flow in conjunction with a body moving through the fluid. These equations represent the viscosity-based fluid flow, taking into account the fluid’s Newtonian nature and the viscous forces’ direct dependence on velocity gradients. A system of partial nonlinear equations is created by these equations working together. When considering water as an incompressible liquid with minor density variations (as indicated in Formula 1), these two equations can be expressed as follows.

$$\frac{\partial U_i}{\partial x_i} = 0$$

$$\rho \frac{\partial U_i}{\partial t} + \rho \frac{\partial(U_i U_j)}{\partial x_i} = \rho R_i + \frac{\partial \sigma_{ij}}{\partial x_j} \quad (1)$$

where  $\rho$  is the water’s density,  $t$  is time,  $\sigma_{ij}$  is the tensor of all tensions, and  $U_i$  is the instantaneous components of fluid velocity in the cartesian coordinate system  $x_i$ . The  $k$ -omega model, first put forth by Wilcox in 1998 and later updated in 2008, is one of the most widely used turbulence models now in use. In this research, two differential equations are utilized in this turbulence model for the two variables  $k$  and  $\omega$ , with the one describing kinetic energy and the second specifying the rate of conversion of kinetic energy into internal heat energy (Umlauf et al., 2003). The two variables have the following Formula 2.

$$\frac{\partial k}{\partial t} + U_i \frac{\partial k}{\partial x_i} = \tau_{ij} \frac{\partial u_i}{\partial x_j} - b^* k \omega + \frac{\partial}{\partial x_i} \left[ (v + S^* v_T) \frac{\partial k}{\partial x_i} \right] \quad (2)$$

$$\frac{\partial \omega}{\partial t} + U_i \frac{\partial \omega}{\partial x_i} = a \frac{\omega}{k} \tau_{ij} \frac{\partial u_i}{\partial x_j} - b \omega^2 + \frac{\partial}{\partial x_j} \left[ (v + S v_T) \frac{\partial \omega}{\partial x_j} \right]$$

The VOF, a numerical approach, is used to specify the free surface demarcation area. The fluid density and viscosity are adjusted in this manner based on a fractional volume function as follows in Formula 3.

$$\mu = \mu_{water} + \mu_{air}(1 - \alpha)$$

$$\rho = \rho_{water} + \rho_{air}(1 - \alpha) \quad (3)$$

where  $\mu_{water}$  and  $\mu_{air}$  refer to the dynamic viscosities of water and air, respectively, and  $\rho_{water}$  and  $\rho_{air}$  refer to the densities of the two fluids (Caramatescu and Mocanu, 2019). The volumetric fraction transport equation, which is calculated for each discrete volume cell in the computation range, controls the location of the liquid’s free surface (as shown in Formula 4).

$$\frac{\partial \alpha}{\partial t} + \nabla(\alpha U) = 0 \quad (4)$$

where  $0 < \alpha < 1$ ,  $U$  is the flow’s speed and the cell’s volume, respectively (Caramatescu and Mocanu, 2019).

Three outcomes can be obtained by solving the equation:

$\alpha = 0$  if the cell is filled with air,

$\alpha = 1$  if the cell is filled with water,

$0 < \alpha < 1$  if the cell has a free surface,

The selection of the  $k$ -omega model has advantages in simulating the hull of the boat. This model is specifically adjusted to its specifications, considering the characteristics of fluid flow in the simulation of the Aceh hull. The VOF approach in CFD was selected for its advantages in accurately simulating free surface flow, offering a level of detail and realism that is often lacking in traditional analytical methods in the complex context of fluid dynamics around the hull of the boat.

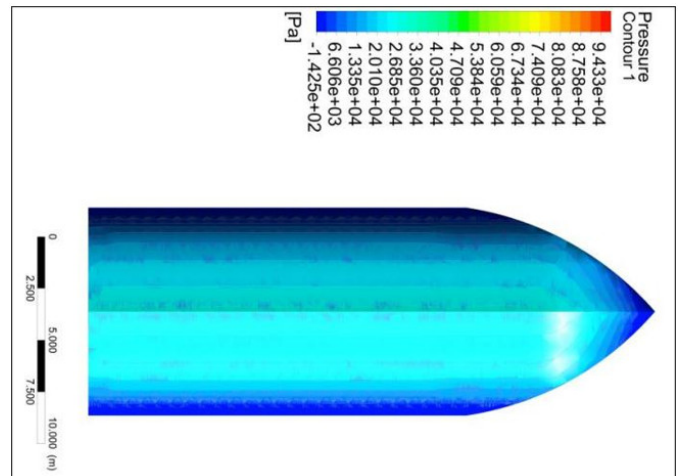
### 3. Results and Discussions.

Figure 4-5, is a collection of figures showing the graphical representation of the pressure distribution determined on a wet surface. The highest pressure gradient is observed at the

stagnation point, which is where the hull enters the water. Subsequently, polynomial interpolation can be used to retrieve numerical data from pressure calculations produced in each hull surface mesh and send it to the CFD program.

The hull design effectively creates an expected air cushion within the semi-tunnel, reducing frictional resistance. Subsequently, at approximately 29.16 knots, according to mass fraction maps, air vortices begin to emerge, and at 40.82 knots, the entire bottom of the boat inside the semi-tunnel separates from the water’s surface. The air cushion inside the semi-tunnel significantly reduces frictional resistance and improves the hull performance but poses problems such as stability and maneuverability. However, these problems can be minimized by combining advanced control systems and the hull design optimization methods.

Figure 4: Distribution of pressure (Pa) with 0 knots of boat speed.

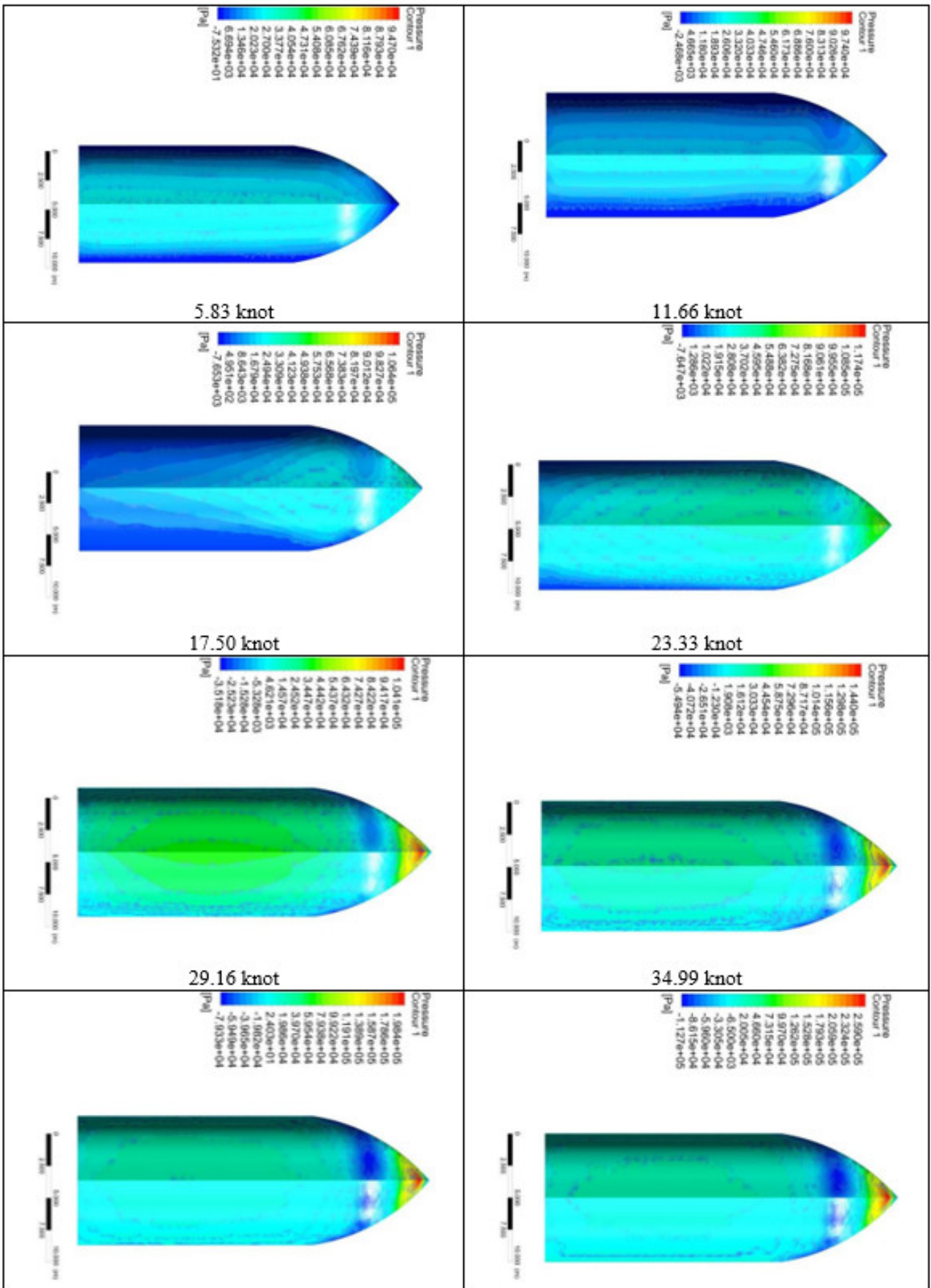


Source: Authors.

Figure 4 shows the pressure distribution on the hull of the Aceh boat at a stop condition or a speed of 0 knots. The color gradation, ranging from dark blue to green is formed along the keel, indicating water pressure from low to high. The maximum visible pressure at the keel is 33.60 kPa. In Figure 5, the pressure distribution on the Aceh boat’s hull is depicted at various speeds, including 5.83, 11.66, 17.50, 23.33, 29.16, 34.99, 40.82, and 46.65 knots. Maximum pressure values are observed along the keel and extended to the side of the hull with values of 47.46, 57.53, 77.50, 81.68, 110.14, 129.8, 178.6, and 259 (in kPa) respectively. The pressure value increases exponentially with increasing speed.

Figure 5 shows the pressure distribution along the hull of the traditional Aceh boat at speeds of 5.83, 11.66, 17.50, 23.33, 29.16, 34.99, 40.82, and 46.65 knots, extending from the keel to the upstream end of the sharp hull area. The maximum pressure values recorded for each of these speeds are 33.60, 47.46, 57.53, 77.50, 81.68, 110.14, 129.8, 178.6, and 259 (in Pa) as shown in Figure 6. At this interval, the maximum pressure value increases sharply with the increase in ship speed. The results are confirmed by a research report under different load-

Figure 5: Distribution of pressure (Pa) with variations in speed: 5.83 to 46.65 knot.



Source: Authors.

ing circumstances and hull thicknesses, this simulation attempts to examine the maximum stress, strain, and displacement of a traditional Aceh fishing boat. The boat was constructed using CNC plate cutting and welding methods. Findings reveal that stress and strain increase with the addition of more loads, and as more weight is placed on the boat's structure, the displacement decreases. The thickness of the steel plate used also plays a role in determining the amount of stress and strain (Akhyar et al., 2021).

The change in trim angle follows the same general trend, increasing during the planning phase and transition period, and then stabilizing and decreasing as speed increases. The predicted trim angles at the estimated start of planning, at 5 m/s, are in close agreement, suggesting that the Savitsky approach provides an accurate estimate for the start of planning (Caramatescu and Mocanu, 2019). Savitsky's approach is a method used to predict the hydrodynamic drag of boat, focusing on the shear resistance of arbitrary hull at low to medium speeds. Some important points about Savitsky's approach include the model of shear resistance, the separation between wet and dry resistance, the Froude Number parameter, and the coefficient of shear resistance. The findings indicated that the bow of the ship's sharp end, which has a pressure of 259 kPa at a boat speed of 46.65 knots, is where the hull is under the most strain. This information will guide the designer in refining the ship's design. Increasing the hull wall thickness can help mitigate damage caused by excessive water pressure at the bow end. In general, the tendency of pressure distribution caused by speed fluctuations is essentially the same; an increase in speed may be observed from the rise in pressure that develops on the ship's hull. In the upstream of Aceh boat, the pressure distribution similarly appears to broaden and migrate from the keel to the pointed end. The assessment of pressure distribution along the hull at different speeds is an essential indicator of hydrodynamic force and loading. This comprehensive understanding enables the optimization of boat design, particularly for the performance of this traditional boat hull. However, the existing design of Aceh fishing boat shows excessively high pressure on the hull, posing a potential risk to safety and structural integrity. Avci and Barlas (2018) reported that simulation on high-speed craft models with the CFD numerical approach can accurately predict resistance, trim, and sinkage calculations, with model towing tank tests validated through experiments. Moreover, addressing ventilation problems through numerical solutions lead to a 27% reduction.

The result shows that the tendency of the pressure distribution remains the same as the speed fluctuations applied. The highest concentration of pressure on the hull at the sharp bow has minimal effect on damages that occur due to the use of fiberglass during the design. Moreover, the manufacturing of composite material has grown rapidly over the years due to its superior properties such as low density, rigidity, and lightweight, including excellent mechanical, and physical properties. The tensile force or strength of materials such as fiberglass can vary based on several factors such as type, material composition, production method, and environmental conditions. Fiberglass generally consists of glass fibers reinforced with polymer resin

/ epoxy. From reference, the highest tensile strength in Glass-Epoxy composites is observed from 330 to 370 MPa, while 270 to 330 MPa for Glass-Vinyl Ester Composites (Singh et al., 2020). The tensile strength of fiberglass-hybrid polyester resin with sand was recorded from 44.84 MPa to 49.49 MPa, which was analyzed by sand size variation (Muchlis et al., 2023). Meanwhile, the highest pressure of Aceh traditional boat from this simulation in the hull at the sharp bow, which was 259 kPa, was lower than the maximum tensile strength value of fiberglass material. Consequently, this value is considered safe for the application of fiberglass material hull for the traditional Aceh boat.

This simulation shows that the highest pressure distribution of the hull occurs at the end of the pointed bow of the Aceh fishing boat design, widening and spreading down due to variations in boat speed. The results show that the highest pressure at high speeds is still safe for gastric applications from fiberglass composite materials because the value of the pressure is significantly below the maximum strength of composite fiberglass.

To anticipate the noise of the material in the high-pressure area, the simulation can also be performed by increasing the thickness in the specific area. The thickness of the traditional Aceh boat hull at the sharp bow should be considered when manufacturing the boat, as indicated by the results of this CFD simulation.

The CFD method is superior to traditional analytical methods in evaluating the behavior of fluid flow around the hull due to its ability to simulate complex fluid pressure more accurately and efficiently. This information is needed by the boat designer in designing to correct errors before the manufacturing process. Analytical methods with potential flow theory or simplified empirical formulas can make it difficult to show complex phenomena detailing fluid flow in the hull area. The dynamic nature of free surfaces, characterized by waves, sparks, and sudden changes in height, presents a formidable challenge to traditional analytical approaches. Predicting the position of free surfaces becomes a complex task, particularly in scenarios where interactions between fluid and structure lead to unstable and unpredictable fluid motion. The CFD method also enables a more realistic representation of fluid flow around the hull of the boat by incorporating actual 3D geometry. This phenomenon facilitates the accurate modeling of complex physics such as turbulence and boundary layer separation, including the simulation of time-dependent and unstable flow conditions.

#### 4. Conclusions and Future Work.

In conclusion, this research analyzed the pressure distribution through the CFD simulation, specifically modeling the traditional Aceh boat hull due to speed variations. The results showed that the numerical simulation appeared to be a tool for analysis with use in the field of marine ship design, as complex geometries could be studied at an early stage of design, enabling engineers to carry out a detailed analysis of the flow field around the ship hull. Subsequently, an evaluation of the value of the CFD analysis was carried out on traditional Aceh boat hulls. The results showed that the maximum pressure on the hull occurred at the sharp end of the bow of the ship, which

was 259 kPa at a boat speed of 46.65 knots. This value drew the designer's attention to improving the ship's design before it was produced. To reduce ship damage due to too high water pressure at the bow end, the hull wall thickness can be increased. The tendency of pressure distribution due to speed variations remained consistent, with increased speed resulting in higher pressure on the ship's hull. The pressure distribution also seems to spread and move from the keel to the pointed end of the upstream of the designed Aceh boat. Based on the numerical CFD simulation conducted to account for variations in ship speed, it is advisable to consider adding thickness to the bow in the design of traditional Aceh boats. This research is limited to analyzing the pressure distribution of the traditional Aceh boat at speed variations of 5.83, 11.66, 17.50, 23.33, 29.16, 34.99, 40.82, and 46.65 knots. For instance, the effects of boat loads, the influence of ocean currents, the use of new materials and technologies (other than fiberglass), modeling ship movement and stability, improving the effectiveness of propulsion, and environmental impacts require further study.

The recommendations for this traditional Aceh boat design in the CFD simulation showed that the tendency of pressure distribution in the hull was the same, without significant change even at maximum speed. The highest pressure from this simulation occurred at the sharp bow, which was below the maximum tensile strength value of the fiberglass material. Therefore, without further modifications to the hull design, the application of the traditional Aceh is considered safe.

### Acknowledgements.

This publication was made possible by a grant from the Research Fund of the Ministry of Research, Technology, and Education, Republic of Indonesia, and the Institute for Research and Community Services (LPPM) Syiah Kuala University; the financial support is greatly appreciated. We would like to thank Mr. Muhammad Fathur Ridha, Mr. Kevin Suherman, and Mrs. Liza Rizqi Handayani for their support during this simulation.

### References.

Avci, A.G., and Barlas. B., 2018. An Experimental and Numerical Study of A High Speed Planing Craft with Full-Scale Validation. *Journal of Marine Science and Technology*, 26(5), pp. 617-628. Available at: [https://doi.org/10.6119/JMST.2018-10.26\(5\).0001](https://doi.org/10.6119/JMST.2018-10.26(5).0001).

Akhyar, Tamlicha, A., Hasanuddin, I., Muchlis, Y., Mubarak, A.M., Azwinur, Yusuf, T.M. and Amri, A., 2021. Numerical Analysis of Traditional Aceh Fishing Boat with Various Scenario Loading and Hull Thickness, Manufacturing by Metal Plasma Cutting and Welding, Proceedings of the 2nd International Conference on Experimental and Computational Mechanics in Engineering, Lecture Notes in Mechanical Engineering, Available at: [https://doi.org/10.1007/978-981-16-0736-3\\_33](https://doi.org/10.1007/978-981-16-0736-3_33).

Azcueta, R., 2003. Steady and unsteady RANSE simulations for planing crafts, Proceedings of the 7th International Conference on Fast Sea Transportation, FAST'03, Ischia, Italy.

Battistin, D., and Iafrati A., 2003. A numerical model for hydrodynamic of planing surfaces. Proceedings of the 7th International Conference on Fast Sea Transportation, FAST'03, Ischia, Italy: 33-38.

Caponnetto, M., 2001. Practical CFD simulations for planing hulls. Proceedings of Second International Euro Conference on High Performance Marine Vehicles, 128-138.

Caramatescu, A., Păcuraru, F., and Cristea, C., 2016. Numerical simulation of a cargo planing boat with inverted keel. International Conference of Traffic and Transport Engineering, ICTTE, Belgrade.

Caramatescu, A., and Mocanu, C.I., 2019. CFD Simulation of A Planing Hull. *International Journal for Traffic and Transport Engineering (IJTTE)*.

Ghassemi, H., and Ghiasi, M., 2008. A combined method for the hydrodynamic characteristics of planing craft. *Ocean Engineering* 35(3-4), pp. 310–322. Available at: <https://doi.org/10.1016/j.oceaneng.2007.10.010>.

Harun, D., Dirhamsyah, M., Fonna, S., Akhyar, Huzni, S., and Tadjuddin, M., 2021. CFD Investigation on Aerodynamic Characteristics and Performance of Windmill Aerator Type Savonius Four Blade. In: Akhyar (eds) Proceedings of the 2nd International Conference on Experimental and Computational Mechanics in Engineering. Lecture Notes in Mechanical Engineering. Springer, Singapore. Available at: [https://doi.org/10.1007/978-981-16-0736-3\\_35](https://doi.org/10.1007/978-981-16-0736-3_35).

Hasanuddin, I., Husaini, Anwar, M.S., Yudha, B.Z.S., and Akhyar, H., 2018. Stress and strain analysis from dynamic loads of mechanical hand using finite element method. IOP Conference Series: Materials Science and Engineering, Vol. 352, 012017, DOI 10.1088/1757-899X/352/1/012017.

Husaini, Putra, D.F., Syahriza, and Akhyar, 2023. Stress and strain analysis of UAV hexacopter frame using finite element method. AIP Conference Proceedings 2613, 020005 (2023); Available at: <https://doi.org/10.1063/5.0119804>.

Iqbal, Ali, N., Husin, H., Akhyar, Khairil, and Farhan, A., 2021. FAE Analysis of Boat Propeller with Differences of Loading Conditions and Manufacturing by Casting Process. In: Akhyar (eds) Proceedings of the 2nd International Conference on Experimental and Computational Mechanics in Engineering. Lecture Notes in Mechanical Engineering. Springer, Singapore. Available at: [https://doi.org/10.1007/978-981-16-0736-3\\_33](https://doi.org/10.1007/978-981-16-0736-3_33).

Kornev, N., and Abbas, N. 2018. Vorticity structures and turbulence in the wake of full block ships. *Journal of Marine Science and Technology*, 23, 567–579. Available at: <https://doi.org/10.1007/s00773-017-0493-3>.

Muchlis, Y., Husaini, Ali, N., and Akhyar. 2023. Evaluation of tensile strength of fibreglass composites-hybrid due to differences in sand size. *Multidisciplinary Science Journal*, 6(6), pp.1-6. Available at: <https://doi.org/10.31893/multiscience.2024085>.

Queutey, P., and Visonneau, M., 2007. An interface capturing method for free-surface hydrodynamic flows. *Computers & Fluids*, 36(9), pp. 1481–1510. Available at: <https://doi.org/10.1016/j.compfluid.2006.11.007>.

Savitsky, D., 1964. Hydrodynamic Design of Planing Hulls. *Marine Technology SNAME* 1(4), pp. 71–95, Available at:

<https://doi.org/10.5957/mt1.1964.1.4.71>.

Savitsky, D., DeLorme, M. F., and Datla, R. 2007. Inclusion of whisker spray drag in performance prediction method for high speed planing hulls, *Marine Technology SNAME*, 4(1), 35–56. Available at: <https://doi.org/10.5957/mt1.2007.44.1.35>.

Singh, M.M., Kumar, H., Kumar, G.H., Sivaiah P., Nagesha. K.V., Ajay K.M., Vijaya. G., 2020. Determination of Strength Parameters of Glass Fibers Reinforced Composites for Engineering Applications. *Silicon*, 12, pp. 1–11. Available at: <https://doi.org/10.1007/s12633-019-0078-3>.

Soupez, J.R.G., 2019. A new ISO 12215-5 for small craft structures, Feature 1 | *Yacht Design and Construction, Ship and*

*Boat International*, pp.1-3.

Umlauf, L., Burchard, H., and Hutter, K., 2003. Extending the  $k-\omega$  turbulence model towards oceanic applications. *Ocean Modelling*, 5(3), pp. 195-218, Available at: [https://doi.org/10.1016/S1463-5003\(02\)00039-2](https://doi.org/10.1016/S1463-5003(02)00039-2).

Wackers, J., and Visonneau, M., 2009. Adaptive grid refinement for ship. flow computation, *Proceedings of ADMOS 2009*, Brussels, Belgium.

Yumin, S., Qingtong, C., Hailong, S., and Wei, L., 2012. Numerical Simulation of a Planing Vessel at High Speed. *Journal of Marine Science and Applications*, 11, pp. 178–183. Available at: <https://doi.org/10.1007/s11804-012-1120-7>.